Echinomycin Binding Sites on DNA

Michael M. Van Dyke and Peter B. Dervan

Abstract. *The preferred binding sites of echinomycin on DNA can be determined by a method called "footprinting." A ^{32}P end-labeled restriction fragment from pBR322 DNA is protected by binding to echinomycin, and cleaved by a synthetic DNA cleaving reagent, methidiumpropyl–EDTA·Fe(II); the DNA cleavage products are then subjected to high-resolution gel analyses. This method reveals that echinomycin has a binding site size of four base pairs. The strong binding sites for echinomycin contain the central two-base-pair sequence 5'-CG-3'. From an analysis of 15 echinomycin sites on 210 base pairs of DNA, key recognition elements for echinomycin are contained in the sequences (5'-3') ACGT and TCGT (A, adenine; C, cytosine; G, guanine; T, thymine).*

A class of small molecules important in antibiotic, antiviral, and antitumor chemotherapy bind in an equilibrium fashion to double-helical deoxyribonucleic acid (DNA) (*1*). Their biological activity is believed related to the formation of this complex with cellular DNA (*1*). The DNA polymer consists of guanine-cytosine (G·C) and adenine-thymine (A·T) base pairs like rungs on a twisted ladder. The shapes of some of these binding drugs are flat, allowing them to sandwich or "intercalate" between the base pairs. Other drugs with less obvious structural features are believed to fit snugly in the minor or major grooves of the right-handed DNA helix by hydrophobic and hydrogen-bonding interactions. For an optimum complementary fit, these "groove binders" must recognize the G·C or A·T base pairs and their surrounding environment. A long-range goal would be a detailed understanding of how these drugs work in man. On the basis of this information, it is not unreasonable to attempt to design more selective and efficient classes of drugs not found in nature. A fundamental first step would be to solve the analytical problem; namely, where on cellular DNA do these molecules bind and what are the optimum base pair combinations or sequence specificities for complexation of these DNA binding drugs.

If intercalators or groove binders bound only one base pair on DNA, that is, one rung on the twisted ladder, the solution to their base sequence preferences would be simple. Comparison of equilibrium binding studies to homopolymer DNA's such as dA·dT or dG·dC would allow us to characterize drugs as G·C or A·T binders (*1*) (dA, dT, dG, dC, deoxyadenylate, deoxythymidylate, deoxyguanylate, and deoxycytidylate). However, the sizes of these drugs are sufficiently large to cover typically two to five contiguous base pairs, up to one half-turn of the DNA helix. Because there are four bases possible for each nucleotide position on each strand in the DNA polymer and within the constraints of the A·T and G·C complementary nature of the DNA helix, we can calculate that binding site sizes of two to five base pairs means that there are 10, 32, 136, and 512 unique combinations of base pairs or specific binding sites on DNA, respectively (*2*).

In 1978 Galas and Schmitz devised a general solution to this problem called "footprinting" which is briefly explained as follows (Fig. 1) (*3*). With the availability of sequence-specific DNA cleaving enzymes (restriction endonucleases) that allow the isolation of discrete DNA fragments 100 to 500 base pairs in size from larger plasmid DNA, we now have available uniform DNA substrates with a sufficiently large number of base pairs or combinations of base pairs to be representative of all possible drug binding sites on DNA. With routine enzymatic procedures, these 100- to 500-bp DNA fragments can be tagged on one end of one strand (5′ or 3′) with the label ^{32}P. In addition, it is known that the DNA cleaving enzyme, deoxyribonuclease I (DNase I), cleaves DNA at every base pair. Although the enzyme is sensitive to DNA structure and cleaves along the DNA polymer at nonidentical rates, for the purposes of this experiment it can be regarded as having relatively low sequence specificity, especially under conditions of what is called single-hit kinetics. After cleavage of a ^{32}P-labeled restriction fragment with DNase I, we can visualize the ladder of the DNA cleavage sites on the autoradiogram by high-resolution gel electrophoresis which resolves the set of cleavage products differing in length by only one base pair. For footprinting, we allow the DNA binding molecules to bind their preferred sequences among the 100 to 500 base pairs available on the DNA restriction fragment, followed by cleavage with DNase I. A bound protein or drug would then "protect" the recognition DNA site from cleavage between the base pairs it covers. This is visualized on the autoradiogram of the high-resolution gel as a gap or light region in the "sequencing ladder"; the gap is due to the missing DNA cleavage products, which are the sites protected from cleavage (Fig. 1). A chemical sequencing lane run alongside as a marker permits precise identification of these protected regions. This technique, called "DNase I footprinting," was first used by Galas and Schmitz to determine the sequence preferences of DNA binding proteins that cover about 20 base pairs or approximately two turns of the DNA helix (*3*).

Attempts to use DNase I footprinting to determine the binding locations of smaller molecules such as the antibiotic, antiviral, and antitumor drugs have been successful, except for one serious drawback. The DNase I footprinting method reveals binding site sizes that are significantly larger than would be expected for small molecules complexed to DNA (*4–6*). For example, from model building the antitumor antibiotic, actinomycin, is expected to cover four base pairs. DNase I footprinting revealed binding sites that were six to nine base pairs in size (*4–6*). Because binding site size is a critical parameter for defining the sequence specificities of small molecules on DNA, a synthetic footprinting tool, called methidiumpropyl–EDTA·Fe(II), was developed which would mimic DNase I as a DNA cleaving reagent and, in addition, afford more accurate resolution of the binding site sizes for DNA binding drugs in footprinting experiments (*5, 7–11*).

Methidiumpropyl-EDTA (MPE) con-

M. M. Van Dyke is a postdoctoral fellow at Rockefeller University, New York 10021. P. B. Dervan is professor of chemistry at the California Institute of Technology, Pasadena 91125.

tains the DNA intercalator, methidium, covalently bound by a short hydrocarbon tether to the metal chelator, ethylenediaminetetraacetate (EDTA) (*7, 8*). In the presence of ferrous ion and oxygen, MPE efficiently produces single-strand breaks in double-helical DNA (*7, 8*). Furthermore, the synthetic MPE·Fe(II) is a relatively nonsequence specific DNA cleaving agent and cleaves DNA with lower sequence specificity than DNase I (*5, 7–11*). With the use of MPE·Fe(II) footprinting, the preferred binding sites and binding site sizes of small molecules such as actinomycin, distamycin, netropsin, chromomycin, mithramycin, and olivomycin on DNA restriction fragments have been determined (*5, 9–11*). Comparisons of MPE·Fe(II) and DNase I footprinting have shown that the resolution of the binding site size of small molecules on DNA appears more accurate with MPE·Fe(II), especially in cases where several drugs are closely spaced on the DNA (*5*).

Some (but not all) drugs upon binding their optimum sequence distort the DNA polymer, for example, by unwinding, or helix extension. The question then arises as to how far on the DNA this drug-induced distortion or alteration of DNA structure extends. Undoubtedly this alteration will be both drug dependent and sequence dependent. It is in this area that DNase I footprinting is now most useful. DNase I is sensitive to DNA structure, and DNase I cleavage should be inhibited or enhanced by altered DNA structure. DNase I footprinting should prove to be a powerful technique for determining the extent and sequence dependence of altered DNA structure induced by small molecules at specific sites on DNA (*4, 5*).

The identification of the preferred binding sites for drugs on native DNA in solution is only a first step to understanding the rules of recognition for complex formation between drugs and DNA. Questions such as how the drug binds in the major or minor groove, what distortions do the drugs impose on the DNA, and what are the key recognition elements on the drug and the DNA helix that afford such a tight complex cannot be answered by footprinting; we must rely on more direct methods such as high resolution x-ray analysis of judiciously chosen drug-oligonucleotide complexes. The number of available crystal structures of drug-DNA complexes are few and a critical mass of comparisons of solution studies with solid-state x-ray analyses are lacking.

It is the purpose of this article to present MPE·Fe(II) footprinting data on the optimum DNA binding sites in solution of the natural product echinomycin. Because an x-ray structure of a similar molecule bound to DNA is presented in the accompanying article (*12*), this is one of those rare opportunities in the field of drug-DNA complexation to compare solution studies with solid-state structure studies.

Table 1. Four-base-pair echinomycin binding sites on pBR322 DNA. Abbreviations: s, strong; m, medium; w, weak.

Fragment	Site (5′–3′)	Location	Binding
517	TCGT	4343–4340	s
517	ACGC	4336–4333	w
517	AGGT	5322–4319	w
517	ATGT	4317–4314	w
517	TGGT	4301–4298	m
517	ACGT	4290–4287	s
517	AGGT	4285–4282	w
517	TCGG	4273–4270	m
167	TCGA	24–27	s
167	GCGG	38–42	s
167	CAGT	53–56	w
167	ACGC	67–70	w
167	CCGT	79–82	w
280	CCGG	410–413	w
280	TCGG	469–472	m

Echinomycin

Echinomycin is a DNA binding molecule that has significant antibiotic, antiviral, and antitumor activity (*13–17*). Structural features that characterize echinomycin are a cyclic octapeptide dilactone, two quinoxaline chromophores, and a thioacetal bridge (*18, 19*) (Fig. 2). Echinomycin is one of the quinoxaline antibiotics and is distinguished as the first reported example of a DNA bis intercalator (*20*). Binding affinities for echinomycin to naturally occurring DNA's of differing base composition vary with a preference for DNA rich in G+C content (*21*). However, the nature of the sequence preferences remains obscure. The highest binding affinity observed was with *Micrococcus lysodeikticus* DNA (72 percent G+C) and not with the copolymer poly[d(G-C)] or the homopolymer poly(dG·dC), suggesting that all four bases in the binding site may be important in the recognition process (*15*). Recent kinetic studies of echinomycin on heterogeneous DNA provides supporting evidence for more than one class of binding sites (*22*). This led Waring and co-workers to estimate that, if

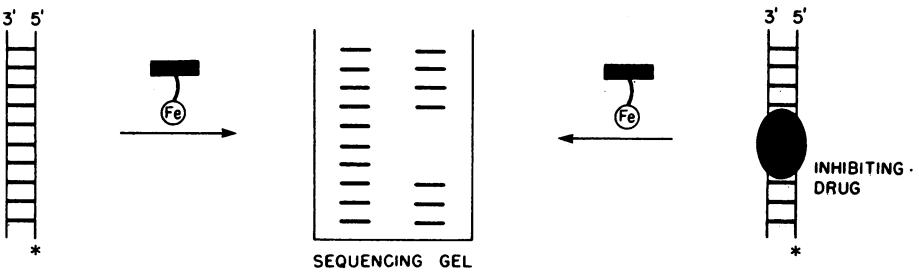

Fig. 1. Illustration of the footprinting technique with MPE·Fe(II) cleavage of drug-protected DNA restriction fragments, followed by analysis with high resolution gel electrophoresis.

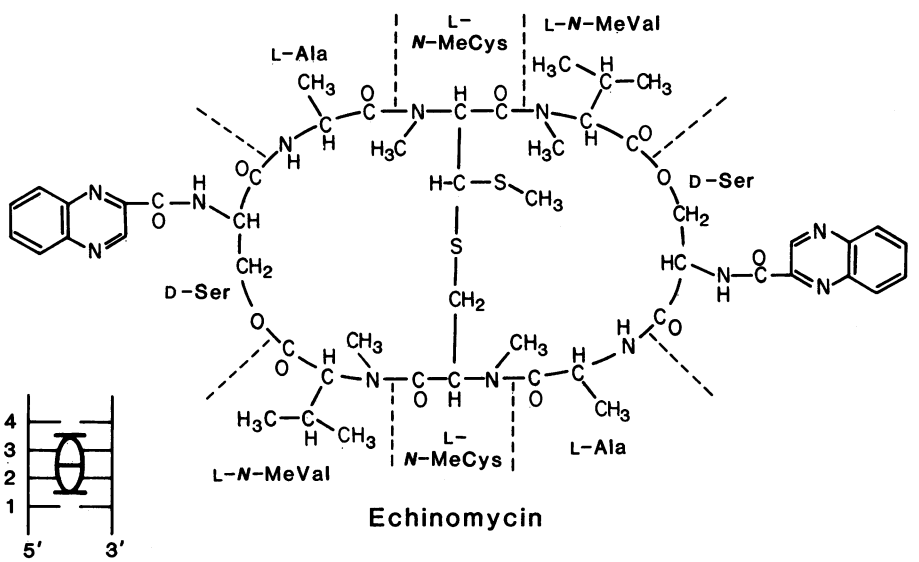

Fig. 2. Formula of echinomycin. The figure at lower left illustrates a bis intercalator bound in the minor groove of DNA bracketing the two central base pairs of a 4-bp binding site.

echinomycin has a binding site size of four base pairs, of the 136 distinguishable permutations, only three or four of these are highly preferred binding sites (*22*). Most likely, part of the sequence-specific binding of echinomycin to DNA involves interactions between the peptide portion of echinomycin and the bases in the minor groove of the DNA helix. One step toward understanding the recognition elements for echninomycin-DNA complexation is the identification of those highly preferred echinomycin binding sites on native DNA.

We have examined the preferred binding sites of echinomycin on 210 base pairs from three restriction fragments from pBR322 plasmid DNA. The MPE·Fe(II) footprinting of echinomycin bound to these DNA fragments from pBR322 plasmid resulted in two major observations. The minimum binding site size for echinomycin is four base pairs, and strong binding sites are 5′-3′ ACGT and TCGT. For comparison, DNase I footprinting of echinomycin affords footprints in similar locations and of larger size.

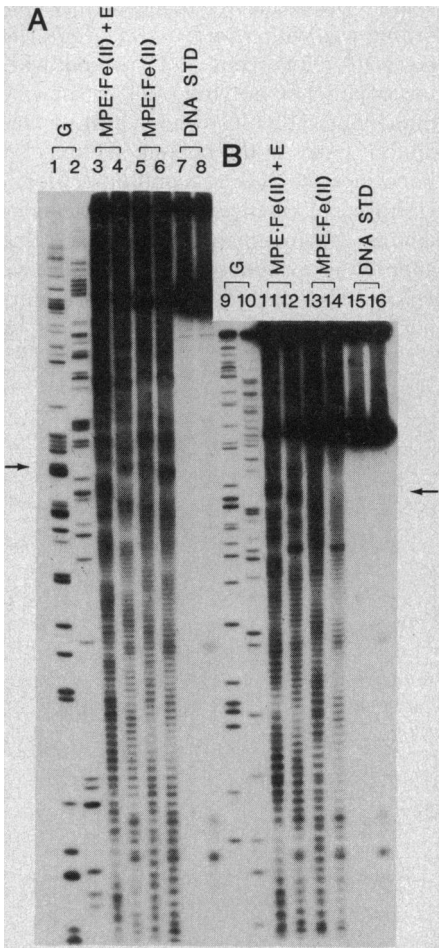

Fig. 3. Autoradiogram of 5′ (odd-numbered lanes) and 3′ (even-numbered lanes) ^{32}P end-labeled DNA restriction fragments. (A) Lanes 1 to 8 are from the 517-bp fragment. (B) Lanes 9 to 16 are from the 167-bp fragment. Lanes 1, 2, 9, and 10 are Maxam-Gilbert chemical sequencing (*28*) G-specific reactions. Lanes 3, 4, 11, and 12 are MPE·Fe(II) footprinting of echinomycin at 200 μ*M*. Lanes 5, 6, 13, and 14 are MPE·Fe(II) cleavage of unprotected DNA. Lanes 7, 8, 15, and 16 are intact DNA. From this autoradiogram 80 base pairs of the 517-bp fragment (lanes 1 to 8) and 70 base pairs of the 167-bp fragment (lanes 9 to 16) have been analyzed by densitometry. The bottom to arrow at the middle of the autoradiogram is the sequence left to right in Fig. 5.

MPE·Fe(II) Footprinting

Footprints produced by partial cleavage of three DNA restriction fragments from plasmid pBR322 protected by echinomycin were examined (*23–27*). A 517-bp (Rsa I–Eco RI), a 167-bp (Eco RI–Rsa I), and a 280/276–bp (Bam HI–Sal I) fragment all appeared to have several strong echinomycin binding sites. The DNA fragments labeled at the 3′ (or 5′) end with ^{32}P were allowed to equilibrate with echinomycin at ratios of echinomycin to DNA base pairs of 0.03 to 0.50 (Figs. 3 and 4). Then MPE·Fe(II) was added to afford a final ratio of MPE·Fe(II) to DNA base pairs of 0.025. The reaction was initiated by the addition of dithiothreitol (DTT) at 4 m*M* concentrations. Cleavage by MPE·Fe(II) was stopped after 15 minutes (37°C) by freezing, lyophilization, and resuspension in formamide buffer. The ^{32}P end-labeled DNA products were analyzed by denaturing gel (8 percent polyacrylamide–50 percent urea) electrophoresis capable of resolving DNA fragments differing in length by one nucleotide. The autoradiogram for MPE·Fe(II) footprinting on the 517-bp and 167-bp fragments is shown in Fig. 3. The autoradiogram for MPE·Fe(II) and DNase I footprinting on the 280/276–bp fragment is shown in Fig. 4.

The 517-bp fragment (Rsa I–Eco RI). Control lanes 7 and 8 (Fig. 3A) are the buffered intact 517-bp restriction fragment of DNA (400 μ*M*, in base pair), 10 μ*M* Fe(II), and 4 m*M* DTT concentrations used in the footprinting reactions. Control lanes 5 and 6 (Fig. 3A) are MPE·Fe(II) cleavage of the 517-bp restriction fragment labeled at the 5′ (or 3′) end with ^{32}P. A relatively uniform DNA cleavage pattern is observed. Lanes 1 and 2 (Fig. 3A) are the Maxam-Gilbert chemical sequencing G lanes used as markers (*28*). Echinomycin was allowed to equilibrate with the 517-bp DNA fragment at a ratio of echinomycin to DNA base pairs of 0.50, followed by partial cleavage with MPE·Fe(II) (Fig. 3A, lanes 3 and 4). From densitometric analyses, the footprints (cleavage inhibition) on 80 bp of the 517-bp DNA fragment are shown in Fig. 5. MPE·Fe(II) cleavage reveals eight binding locations four base pairs in size (Fig. 5 and Table 1).

The 167-bp fragment (Eco RI–Rsa I). Control lanes 15 and 16 (Fig. 3B) are the buffered intact 167-bp restriction fragment of DNA (400 μ*M*, in base pair), 10 μ*M* Fe(II), and 4 m*M* DTT concentrations used in the footprinting reactions. Control lanes 13 and 14 (Fig. 3B) are MPE·Fe(II) cleavage of the 167-bp restriction fragment labeled at the 5′ (or 3′) end with ^{32}P. A relatively uniform DNA cleavage pattern is observed. Lanes 9 and 10 (Fig. 3B) are the chemical

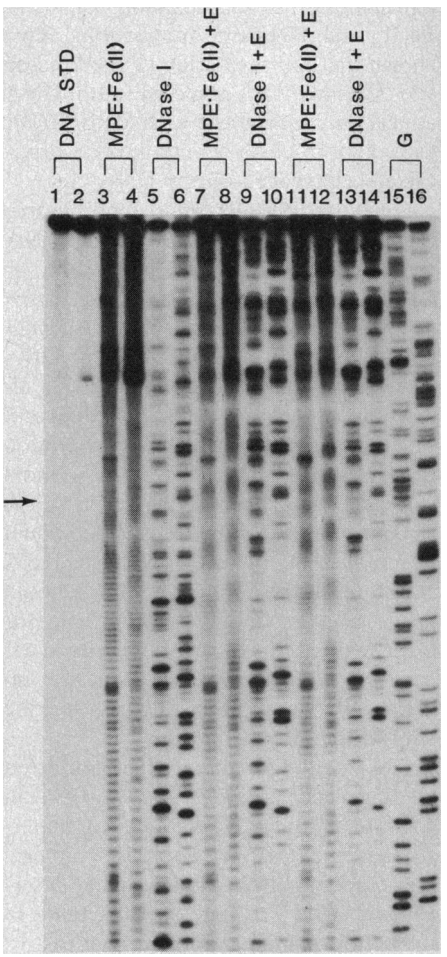

Fig. 4. Autoradiogram of 3′ (odd-numbered lanes) and 5′ (even-numbered lanes) ^{32}P end-labeled 280/276–bp DNA restriction fragment. Lanes 1 and 2, intact DNA; lanes 3 and 4, MPE·Fe(II) cleavage of unprotected DNA; lanes 5 and 6, DNase I cleavage of unprotected DNA; lanes 7 and 8, MPE·Fe(II) footprinting of echinomycin at 12 μ*M*; lanes 9 and 10, DNase I footprinting of echinomycin at 12 μ*M*; lanes 11 and 12, MPE·Fe(II) footprinting of echinomycin at 48 μ*M*; lanes 13 and 14, DNase I footprinting of echinomycin at 50 μ*M*; lanes 15 and 16, Maxam-Gilbert chemical sequencing G-specific reaction. From this autoradiogram, 70 base pairs have been analyzed by densitometry. Bottom to arrow at the middle of the autoradiogram is the sequence left to right in Fig. 6.

sequencing G lanes used as markers. Echinomycin was allowed to equilibrate with the 167-bp DNA fragment at a ratio of echinomycin to DNA base pairs of 0.50, followed by partial cleavage with MPE·Fe(II) (Fig. 3B, lanes 11 and 12). From densitometric analyses, the footprints on 70 bp of the 167-bp DNA fragment are shown in Fig. 5. Cleavage with MPE·Fe(II) reveals five binding locations four base pairs in size (Fig. 5 and Table 1).

The 280/276–bp fragment (Bam HI–Sal I). Control lanes 1 and 2 (Fig. 4) are the buffered intact 280/276–bp restriction fragment of DNA (400 μM in base pair), 10 μM Fe(II), and 4 mM DTT concentrations used in subsequent footprinting reactions. Control lanes 3 and 4 (Fig. 4) are MPE·Fe(II) cleavage of the 280/276–bp restriction fragment labeled at the 3′ (or 5′) end with ^{32}P. A relatively uniform DNA cleavage pattern is observed. DNase I cleavage exhibits a higher sequence specificity shown in lanes 5 and 6 (Fig. 4). Lanes 15 and 16 (Fig. 4) are Maxam-Gilbert (*28*) chemical sequencing G lanes used as markers. Echinomycin was allowed to equilibrate with the 280/276–bp DNA fragment at a ratio of echinomycin to DNA base pairs of 0.03, followed by partial cleavage with MPE·Fe(II) (Fig. 4, lanes 7 and 8) or DNase I (Fig. 4, lanes 9 and 10). From densitometric analyses the footprints on 60 bp of the 280/276–bp DNA fragment are shown in Fig. 6, A and B. For echinomycin at low binding density, MPE·Fe(II) cleavage affords four footprints, which are four, six, nine, and four base pairs in size (reading 5′ → 3′ on the top strand of Fig. 6A). DNase I cleavage affords four footprints in the same locations which are larger in size; 6, 8, 20, and 5 base pairs in size (reading 5′ → 3′ on the top strand of Fig. 6A). Echinomycin was allowed to equilibrate with the 280/276–bp DNA fragment at a ratio of echinomycin to DNA base pairs of 0.12, followed by partial cleavage with MPE·Fe(II) (Fig. 4, lanes 11 and 12) or DNase I (Fig. 4, lanes 13 and 14). In addition to the four footprints observed at the lower concentrations, an additional footprint six base pairs in size appears (Fig. 6B). DNase I detected this site at the lower echinomycin concentrations.

Discussion

Assignment of binding site size of echinomycin from MPE·Fe(II) footprinting is based on a model where the DNA cleavage inhibition pattern is shifted one to two base pairs on the 3′ side and is one base pair underprotected on the 5′ side of the DNA (*10, 11*). The minimum binding site size for echinomycin by MPE·Fe(II) footprinting is four base pairs. This is consistent with the average binding site size (four to six base pairs) calculated from equilibrium binding studies (*20, 21*) as well as CPK (Corey,

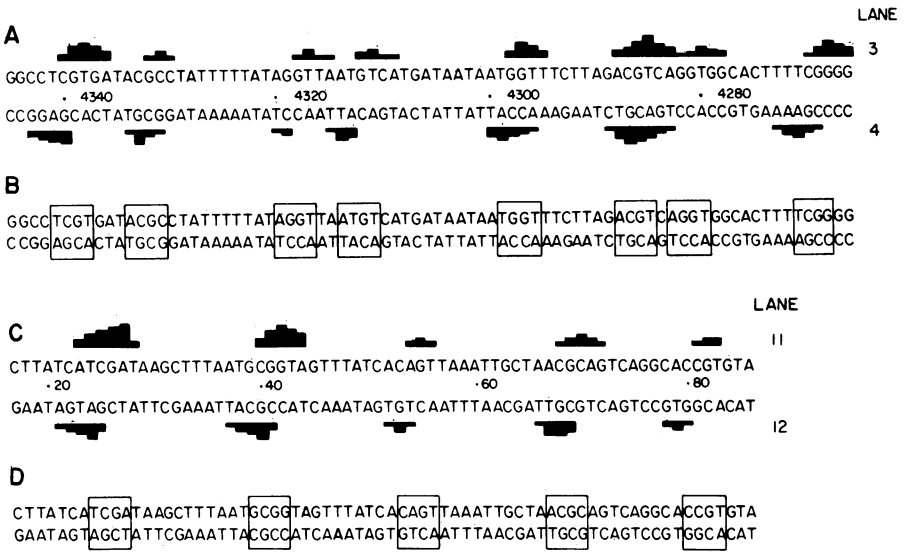

Fig. 5. MPE·Fe(II) footprints of echinomycin at 200 μM concentration on 80 and 70 base pairs of the 517-bp and 167-bp restriction fragments, determined by densitometry from the autoradiogram in Fig. 3. The MPE·Fe(II) footprints (light regions in the gel autoradiogram, Fig. 3) are shown as histograms, the height is proportional to the reduction of cleavage at each nucleotide compared with the MPE·Fe(II) cleavage of unprotected DNA (see control lanes 5, 6, 13, and 14 in Fig. 3). The top strand patterns are for 5′ end-labeled DNA; the bottom strand patterns are for 3′ end-labeled DNA. Boxes are the echinomycin binding sites as suggested on the asymmetric MPE·Fe(II) footprinting model (*10, 11*). (A) and (B) are from the 517-bp restriction fragment. (C) and (D) are from the 167-bp restriction fragment.

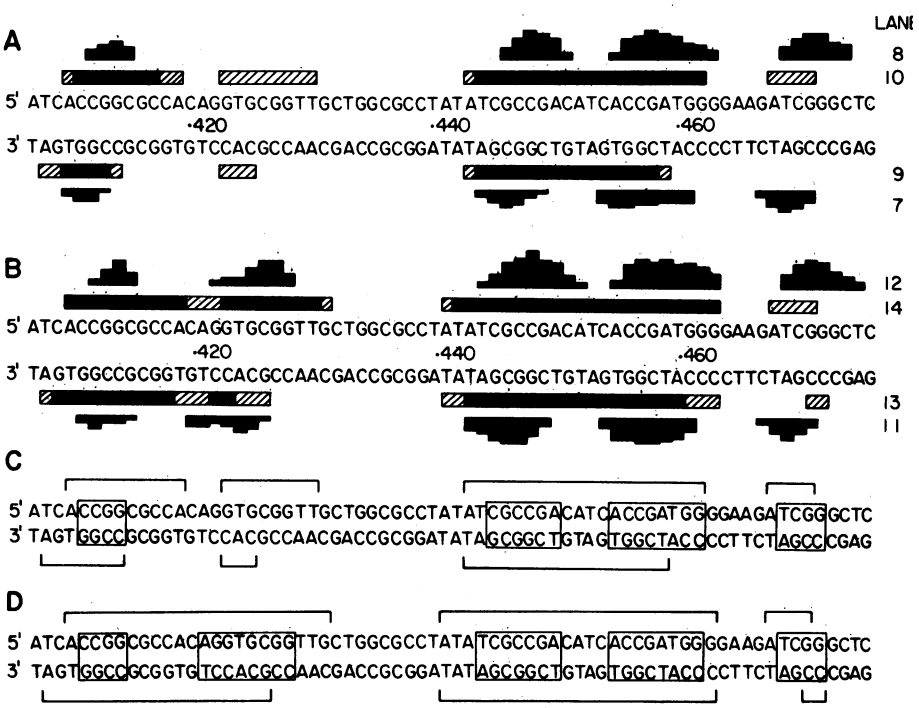

Fig. 6. MPE·Fe(II) and DNase I footprints of echinomycin at (A and C) 12 μM and at (B and D) 48 μM concentrations on 70 base pairs of the 280/276–bp fragment determined by densitometry from autoradiogram in Fig. 4. MPE·Fe(II) footprints (light regions in the gel autoradiogram) are shown as histograms; the height is proportional to the reduction of cleavage at each nucleotide compared with the MPE·Fe(II) cleavage of unprotected DNA (see control lanes 3 to 4 in Fig. 4). DNase I–DNA cleavage inhibition is shown by light and dark bars, corresponding to partial and complete cleavage inhibition, respectively. Top strand patterns are for 5′ end-labeled DNA; bottom strand patterns are for 3′ end-labeled DNA. Boxes are echinomycin binding sites from MPE·Fe(II) footprints (Fig. 4) based on the MPE·Fe(II) footprinting model (*10, 11*). Brackets are DNase I footprints on each strand for comparison.

Prelog, Koltun) space-filling model building studies of the echinomycin·DNA complex. Therefore, we assume that the occurrence of a footprint four base pairs in size corresponds only to one echinomycin site. On the 210 base pairs examined there are 15 echinomycin sites that are four base pairs in size (Table 1).

If the 15 echinomycin binding sites that are four base pairs in size are weighted equally, we find that the first base pair of the tetramer (reading 5′ to 3′) has sequence preference (in decreasing order) A,T > C,G; the second base is C >> G > A,T; the third base is G in all cases; and the fourth base is T > G > C,A. From this limited set of data one would conclude that optimum sequences for echinomycin binding would be 5′-TCGT-3′ and 5′-ACGT-3′. By qualitatively grouping the 15 sites as strong, medium, and weak from the intensity of the MPE·Fe(II) footprint, we find that the strong echinomycin sites appear to be (5′-3′) TCGT, ACGT, TCGA, and GCGG. All strong sites contain the central sequence 5′-CG-3′ (Table 1).

The echinomycin binding sites larger than four base pairs observed by MPE·Fe(II) footprinting are more difficult to interpret (Fig. 6). We presume that these represent regions of close multiple or overlapping binding sites for echinomycin. The larger MPE·Fe(II) footprints for echinomycin are, 5′-AGGTGCGG-3′ (bp, 421 to 428), 5′-TCGCCGA-3′ (bp, 444 to 450), and 5′-ACCGATGG-3′ (bp, 455 to 462) (Fig. 6D). If we presume from the four base pair sites that the central sequence 5′-CG-3′ is a key recognition element in the binding of echinomycin to DNA, one interpretation of the data is that the seven-base-pair site 5′-TCGCCGA-3′ (bp, 440 to 450) is the result of two overlapping echinomycin sites 5′-*TCGC*(CGA)-3′ and 5-(TCG)*CCGA*-3′. Similarly, the eight-base-pair site 5′-ACCGATGG-3′ (bp, 455 to 462) could be the result of overlapping 5′-(A)*CCGA*(TGG)-3′ and 5′-(ACCG)*ATGG*-3′ (Fig. 6). In this latter case, the two-base-pair sandwich rule of 5′-CG-3′ in the center appears to relax to 5′-TG-3′. Finally, the eight-base-pair site 5′-AGGTGCGG-3′ (bp, 421 to 428) that appears at higher echinomycin concentrations could be the result of 5′-(AGGT)*GCGG*-3′ and 5′-*AGGT*(GCGG)-3′.

For echinomycin, DNase I footprinting provides larger binding site sizes than MPE·Fe(II), especially in cases where several binding sites are closely spaced on DNA (Fig. 6). This is implied by the smaller and multiple discrete footprints observed with MPE·Fe(II) cleavage which more closely resembled the expected binding site size of echinomycin on DNA (Fig. 6). The difference in the size of the echinomycin footprints generated by DNase I and MPE·Fe(II) may be a reflection of the differences in the size of the DNA cleaving agents. The synthetic MPE, an intercalator, is significantly smaller than DNase I, a high molecular weight protein. MPE·Fe(II) footprints might simply represent regions of the DNA where echinomycin directly inhibits intercalation by MPE. The catalytic site on the enzyme DNase I might not be accessible to the unprotected base pairs immediately flanking echinomycin in the minor groove of DNA affording a slightly larger footprint. Because DNase I is known to be sensitive to DNA structure (*29*), an alternative explanation for the larger binding site sizes for DNase I footprints is that the DNase I cleavage could be either inhibited or enhanced by altered DNA structure contiguous to the echinomycin binding site.

In summary, MPE·Fe(II) footprinting of echinomycin on native DNA from pBR322 reveals a binding site size of four base pairs. Footprinting reveals that the sequences (5′-3′) TCGT and ACGT are preferred recognition sites for echinomycin (Table 1). The three-dimensional structure of a complex between the quinoxaline antibiotic, triostin A, and a DNA duplex, 5′-CGTACG-3′ has recently been solved by Rich and his co-workers (*12*). They find direct evidence that triostin A is a bis intercalator that brackets a two-base-pair sandwich 5′-CG-3′, forming three important hydrogen bonds between the L-alanine of the octapeptide backbone of triostin A and the guanine (G) in the minor groove of DNA (*12*). The NH groups of both alanine residues on triostin A form hydrogen bonds to the guanine (G) on opposite and adjacent base pair residues of the DNA duplex. However, only one carbonyl of the two alanines forms a hydrogen bond to guanine, suggesting that recognition of triostin A on opposite strands of DNA is unequal (*12*). In addition, they made the remarkable observation that the A·T base pairs on the outside of the intercalation site are rearranged from Watson-Crick to Hoogsteen pairing (*12*). The antibiotics echinomycin and triostin A are structurally similar. They share the same quinoxaline rings and octapeptide ring. Echinomycin differs from triostin A only in the cross bridge, thioacetal in the former and disulfide in the latter. The Rich group has also found that crystals of the complex of echinomycin and 5′-CGTACG-3′ have the same diffraction pattern as the complex of triostin A and 5′-CGTACG-3′, an indication that its structure may be the same (*12*). If this is true, the crystal structure of the complex of triostin A and DNA explains the footprinting data of echinomycin on DNA in solution with regard to the size of the binding site, the importance of the central 5′-CG-3′, and the possible fate of the A·T base pair capping the four-base-pair binding site.

References and Notes

1. E. F. Gale, C. Cundliffe, P. E. Reynolds, M. H. Richmond, M. J. Waring, in *The Molecular Basis of Antibiotic Action* (Wiley, New York, 1981), pp. 258–401.
2. D. Crothers, private communication.
3. D. J. Galas and A. Schmitz, *Nucleic Acids Res.* **5**, 3157 (1978).
4. M. Lane, J. C. Dabrowiak, J. N. Vournakis, *Proc. Natl. Acad. Sci. U.S.A.* **80**, 3260 (1983).
5. M. W. Van Dyke and P. B. Dervan, *Nucleic Acids Res.* **11**, 5555 (1983).
6. A. V. Scamrov and R. Sh. Beabealashvilli, *FEBS Lett.* **164**, 97 (1983).
7. R. P. Hertzberg and P. B. Dervan, *J. Am. Chem. Soc.* **104**, 313 (1982).
8. ———, *Biochemistry*, in press.
9. M. W. Van Dyke *et al.*, *Proc. Natl. Acad. Sci. U.S.A.* **79**, 5470 (1982).
10. M. W. Van Dyke and P. B. Dervan, *Cold Spring Harbor Symp. Quant, Biol.* **47**, 347 (1982).
11. ———, *Biochemistry* **22**, 2373 (1983).
12. A. H.-J. Wang, G. Ughetto, G. J. Quigley, T. Hakoshima, G. A. van der Marel, J. H. van Boom, A. Rich, *Science* **225**, 1115 (1984).
13. D. C. Ward, E. Reich, I. H. Goldberg, *ibid.* **149**, 1259 (1965).
14. K. Sato, O Shiratori, K. J. Katagiri, *J. Antibiot. Ser. A* **20**, 270 (1967).
15. M. Waring and A. Makoff, *Mol. Pharmacol.* **10**, 214 (1974).
16. K. Katagiri, T. Yoshida, K. Sato, in *Antibiotics*, vol. 3, *Mechanism of Action of Antimicrobial and Antitumor Agents*, J. W. Corcoran and F. E. Hahn, Eds. (Springer-Verlag, Heidelberg, 1975), p. 234.
17. M. J. Waring, in *Antibiotics*, vol. 5, *Mechanism of Action of Antieukaryotic and Antiviral Compounds*, F. E. Hahn, Ed. (Springer-Verlag, Berlin, 1979), part 2, pp. 173–194.
18. A Dell, D. H. Williams, H. R. Morris, G. A. Smith, J. Feeney, G. C. K. Roberts, *J. Am. Chem. Soc.* **97**, 2497 (1975).
19. D. G. Martin, S. A. Mizsak, C. Biles, J. C. Stewart, L. Baczynskyj, P. A. Meulman, *J. Antibiot.* **28**, 332 (1975).
20. M. J. Waring and L. P. G. Wakelin, *Nature (London)* **252**, 653 (1974).
21. L. P. G. Wakelin and M. J. Waring, *Biochem. J.* **157**, 721 (1976).
22. K. R. Fox, L. P. G. Wakelin, M. J. Waring, *Biochemistry* **20**, 5764 (1981).
23. Echinomycin was obtained from the Natural Products Branch, Division of Cancer Treatment, National Cancer Institute. Methidiumpropyl-EDTA was synthesized and purified as described (*7*, *8*). $Fe(NH_4)_2(SO_4)_2{\cdot}6\ H_2O$ was obtained from Baker and dithiothreitol (DTT) was obtained from Calbiochem. Aqueous 5′-[α-^{32}P]dATP triethylammonium salt (dATP, deoxyadenosine triphosphate), 3000 Ci/mmol, was from Amersham and aqueous 3′-[γ-^{32}P]dATP, 5000 to 9000 Ci/mmol, was from ICN. The nucleotide triphosphates were from Boehringer Mannheim. All enzymes were from New England Biolabs except bacterial alkaline phosphatase and T4 polynucleotide kinase, which were from BRL. Solutions of $Fe(NH_4)_2(SO_4)_2$, DTT, and MPE were freshly prepared before use. Echinomycin and MPE were characterized spectroscopically before use. MPE was mixed with $Fe(NH_4)_2(SO_4)_2$ at 1 m*M* concentrations immediately before use, and diluted appropriately. The DNA was isolated from the bacterial plasmid pBR322 whose entire sequence is known (*30*). Milligram quantities of the plasmid were grown in *Escherichia coli* strain HB 101 and isolated by procedures similar to those of Tanaka and Weisblum (*31*). Calf thymus DNA (Sigma) was deproteinized and extensively dialyzed.

24. Preparation of specifically labeled DNA fragments. Superhelical pBR322 plasmid DNA was digested with the restriction endonuclease Eco RI and then labeled at the 3′ end with [α-^{32}P]dATP, with the Klenow fragment of DNA polymerase I. A second enzymatic digest with the restriction endonuclease Rsa I yielded two 3′ end-labeled DNA fragments, 167 and 517 base pairs in length. These fragments were isolated by gel electrophoresis on a 5 percent polyacrylamide gel, 1:30 cross-linked, 2 mm thick. Isolation of the fragments from the gel and subsequent procedures were similar to those of Maxam and Gilbert (*28*). Cleavage of pBR322 with Eco RI and successive treatment with bacterial alkaline phosphatase, [γ-^{32}P]ATP and T4 polynucleotide kinase (*28*) and restriction with Rsa I yielded the 167- and 517-bp DNA fragment labeled with ^{32}P at the 5′ end. The 280-bp fragment labeled at the 3′ end and 276-bp fragment labeled at the 5′ end were obtained by similar procedures with Bam HI followed by Sal I restriction enzyme digests.
25. DNA cleavage reactions with MPE·Fe(II). Each reaction initially consisted of a solution (7 μl) of 14 m*M* tris (*p*H 7.4), 70 m*M* NaCl, and 560 μ*M* DNA (base pairs); the DNA was composed of 3′-^{32}P (or 5′-^{32}P) end-labeled restriction fragment and carrier DNA from calf thymus. To this reaction mixture was added 1 μl of a solution of echinomycin in THF; this mixture was incubated for 15 minutes at room temperature; 1 μl of 100 μ*M* MPE·Fe(II) (freshly prepared from stock) was then added and incubation was continued for 15 minutes at room temperature. Addition of 1 μl of freshly prepared 50 m*M* DTT initiated the cleavage reaction. Final concentrations in the 10-μl reaction volume (90 percent aqueous and 10 percent THF) are 10 m*M* tris (*p*H 7.4), 50 m*M* NaCl, 4 m*M* DTT, 400 μ*M* DNA base pairs and 10 μ*M* MPE·Fe(II). Echinomycin concentrations (12, 48, and 200 μ*M*) were adjusted as specified in the figure legends. Each reaction was stopped after 15 minutes at 37°C, by freezing in dry ice; the mixtures were then lyophilized and resuspended on a formamide buffer for gel electrophoresis.
26. DNA cleavage reactions with DNase I. DNA and echinomycin at the same final concentration as above were allowed to equilibrate at room temperature in a buffer consisting of 10 m*M* tris (*p*H 7.9), 10 m*M* KCl, 10 m*M* $MgCl_2$, and 10 m*M* $CaCl_2$. Cleavage was initiated by addition of 4 ng of DNase I in 0.1 m*M* DTT with a final volume of 10 μl. Cleavage was terminated after 30 seconds by the addition of 2.5 μl of 3*M* ammonium acetate, 0.25*M* EDTA DNase terminating solution, and ethanol precipitation.
27. Sequencing gels. Resolution of the DNA cleavage inhibition patterns was achieved by electrophoresis on 0.4 mm thick, 40 cm long, 8 percent polyacrylamide, 1:20 cross-linked sequencing gels containing 50 percent urea. Electrophoresis was carried out at 1000 V for 3.5 hours to sequence 70 nucleotides, beginning 20 nucleotides from the 3′ (or 5′) labeled end. Autoradiography was carried out at −50°C without the use of intensification screen. A copy (8 by 10 inches) of the original autoradiogram was scanned at 485 nm with the incident beam collimated to a width of 0.2 nm on a Cary 219 spectrophotometer. The data were recorded as the absorbance relative to the film base density and analyzed with the use of an Apple microcomputer.
28. A. M. Maxam and W. Gilbert, *Methods Enzymol.* **65**, 499 (1980).
29. G. P. Lomonosoff, P. J. G. Buttler, A. Klug, *J. Mol. Biol.* **149**, 745 (1981).
30. R. J. Roberts, *Nucleic Acid Res.* **11**, r135 (1983).
31. T. Tanaka and B. Weisblum, *J. Bacteriol.* **121**, 354 (1974).
32. Supported by the American Cancer Society research grant number NP-428, an unrestricted grant from Burroughs Wellcome Co. (P.B.D.), and a National Research Service Award (GM-07616) (to M.W.V.). We thank Dr. A. Rich for informing us of his results before publication. Address correspondence to P.B.D.

8 May 1984; accepted 28 June 1984

AAAS–Newcomb Cleveland Prize
To Be Awarded for an Article or a Report Published in *Science*

The AAAS–Newcomb Cleveland Prize is awarded annually to the author of an outstanding paper published in *Science*. The 1984 competition starts with the 6 January 1984 issue of *Science* and ends with the issue of 21 December 1984. The value of the prize is $5000; the winner also receives a bronze medal.

Reports and Articles that include original research data, theories, or syntheses and are fundamental contributions to basic knowledge or technical achievements of far-reaching consequence are eligible for consideration for the prize. The paper must be a first-time publication of the author's own work. Reference to pertinent earlier work by the author may be included to give perspective.

Throughout the year, readers are invited to nominate papers appearing in the Reports or Articles sections. Nominations must be typed, and the following information provided: the title of the paper, issue in which it was published, author's name, and a brief statement of justification for nomination. Nominations should be submitted to the AAAS–Newcomb Cleveland Prize, AAAS, 1515 Massachusetts Avenue, NW, Washington, D.C. 20005. Final selection will rest with a panel of distinguished scientists appointed by the Board of Directors.

The award will be presented at a session of the AAAS annual meeting. In cases of multiple authorship, the prize will be divided equally between or among the authors.

Echinomycin Binding Sites on DNA

Michael M. Van Dyke and Peter B. Dervan

Science, **225** (4667), .
DOI: 10.1126/science.6089341